

Mixed state properties of $\text{Bi}_2\text{Sr}_2\text{Ca}_2\text{Cu}_3\text{O}_{10+\delta}$ single crystals before and after neutron irradiation

M. Weigand,¹ M. Eisterer,^{1,*} E. Giannini,² and H. W. Weber¹¹*Institute of Atomic and Subatomic Physics, Vienna University of Technology, 1020 Vienna, Austria*²*Département de Physique de la Matière Condensée, Université de Genève, 24 Quai Ernest-Ansermet, 1211 Geneva, Switzerland*

(Received 2 November 2009; revised manuscript received 16 December 2009; published 20 January 2010)

The reversible and irreversible mixed state parameters of $\text{Bi}_2\text{Sr}_2\text{Ca}_2\text{Cu}_3\text{O}_{10+\delta}$ (Bi-2223) single crystals were determined by magnetic measurements. One of the samples was exposed to fast neutron radiation in order to investigate the influence of defects introduced into the Bi-2223 matrix. We find that irradiation increases (to a varying extent) the critical current density J_c over almost the whole field and temperature range analyzed, in particular also at low B . This differs from tapes where a J_c enhancement was only found at elevated fields. Irradiation also shifted the irreversibility line to higher values and led to an increase in both the magnetic penetration depth λ_{ab} and the upper critical field H_{c2} . These two parameters have been calculated with the help of a model that takes thermal fluctuations of vortices into account. H_{c2} , however, would be expected to decrease according to theoretical predictions for d -wave superconductors. The discrepancy is discussed and requires further investigations.

DOI: [10.1103/PhysRevB.81.014516](https://doi.org/10.1103/PhysRevB.81.014516)

PACS number(s): 74.25.Ha, 74.25.Sv, 74.62.Dh, 74.25.Op

I. INTRODUCTION

In the $\text{Bi}_2\text{Sr}_2\text{Ca}_{n-1}\text{Cu}_n\text{O}_{2n+4+\delta}$ (BSCCO) family, where $n=1, 2$, or 3 , the three-layer compound with $n=3$ (termed Bi-2223 in this paper) is the most interesting superconductor. It shows the highest transition temperature (about 110 K) and critical current density. Bi-2223, however, is only stable in a narrow O_2 pressure and temperature range, which—together with the incongruent melting of its constituents—makes it very hard to synthesize. Only in the last few years different groups succeeded in growing large and phase-pure single crystals with a sharp superconducting transition.^{1–3} These high-quality samples finally allow the investigation of *intra*-granular current transport in Bi-2223 and its pinning properties, which is essential to improve the performance of Bi-based wires and tapes. In the latter the critical current density J_c is limited in a large temperature and field range by grain boundaries, rather than by pinning within the grains. It is thus instructive to compare tapes to single crystals, where the effect of grain boundaries is eliminated.

It is particularly interesting to examine the changes in the superconducting properties due to the introduction of crystal defects which act as artificial pinning centers. Neutron irradiation enabled us to do so while having control over the defect density through the neutron fluence.

In this contribution we report on magnetic measurements on Bi-2223 single crystals before and after neutron irradiation. We will give a brief introduction to our experimental setup and the evaluation methods in Sec. II, followed by results on the critical current density, the irreversibility line, and the reversible parameters in Sec. III.

II. EXPERIMENTAL

The magnetic properties of two Bi-2223 single crystals (labeled H5a and W002) grown by the traveling solvent floating zone technique³ were investigated before and after neutron irradiation. The dimensions of the two samples were between 850 and 1800 μm in the crystallographic ab plane

and 14 and 21 μm in the c direction. Their high quality had been confirmed previously by x-ray diffraction measurements performed on samples grown in the same way.³

A. Critical temperature

The critical temperature T_c was determined from measurements of the magnetic moment vs temperature $m(T)$ in an ac field $H\parallel c$ (amplitude of 30 μT and frequency of 31 Hz) by a Quantum Design 1 T superconducting quantum interference device (SQUID), as shown in Fig. 1. T_c was obtained as the intersection of two tangents to the slope of the transition and the normal conducting range.

B. Hysteresis loops and critical current densities

Magnetic hysteresis loops were measured in an Oxford Instruments vibrating sample magnetometer (VSM) for fields up to 5 T. By approximating the samples as rectangular platelets and using the Bean model,⁴ the critical current density for applied fields $H\parallel c$ was calculated via $J_c(H) = \{m_i(H)/V\} \{4/[b(1-b/3a)]\}$. m_i denotes the irreversible magnetic moment, obtained from moments measured in increasing (m_+) and decreasing (m_-) fields via

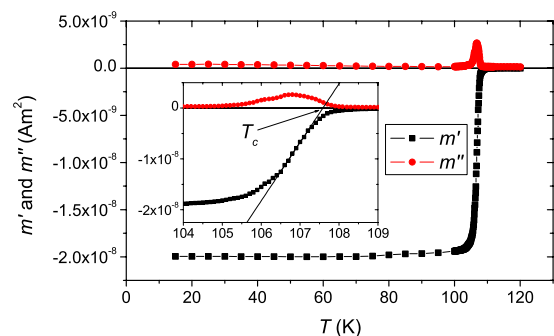


FIG. 1. (Color online) In-phase and out-of-phase components of the magnetic moment vs temperature in an ac field for sample W002 before irradiation.

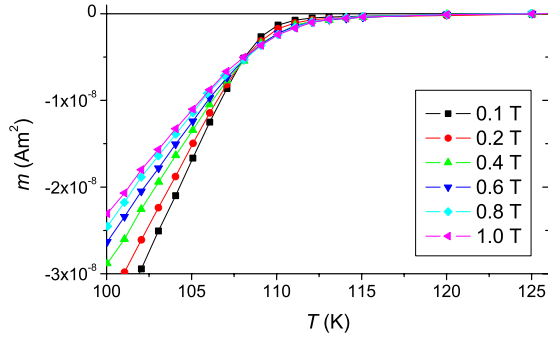


FIG. 2. (Color online) Magnetic moment vs temperature at different applied fields $H\parallel c$ showing the typical crossing point due to thermal fluctuations of vortices for sample W002 before irradiation.

$m_i = (m_+ - m_-)/2$, and V is the volume of the sample with dimensions a , b , and c . The induction B was numerically calculated from $J_c(H)$, which led to values of $J_c(B)$.

C. Irreversibility line

The irreversibility line was determined from magnetic moment vs temperature $m(T)$ curves for $H\parallel c$ measured in a Quantum Design 7 T SQUID (see inset of Fig. 6). First the sample was cooled in zero applied magnetic field [zero field cooled (zfc)] and subsequently a field was set and the temperature increased beyond the expected irreversibility temperature T_{irr} while the magnetic moment was measured in 1 K steps. Immediately afterward a field-cooled (fc) curve down to temperatures below T_{irr} was obtained. This process was repeated for different fields between 0.1 and 7 T.

Each of these curves showed two distinct features: the drifting apart of the zfc and fc branches at $T=T'$ and a kink at a temperature a few kelvins above, a behavior reported previously for $\text{YBa}_2\text{Cu}_3\text{O}_7$ (YBCO) single crystals by Schilling *et al.*⁵ In their study they compared $m(T)$ curves obtained in a SQUID by a conventional method where the sample was moved through the detection coils to the SQUID response voltage when the sample remained at a fixed position. The temperature where the kink was found in $m(T)$ curves acquired by moving the sample corresponded to the irreversibility temperature T_{irr} obtained by the latter method. They claimed that the data for temperatures below T_{irr} are affected by field inhomogeneities and therefore do not correspond exactly to the true moment, which leads to the occurrence of the kink. As a consequence in the present work the temperature of the kink (and not the drifting apart of the zfc and fc curves) was taken as the transition from reversible to irreversible behavior at the respective magnetic field.

D. Reversible properties

The reversible properties were determined using a model developed by Bulaevskii *et al.*⁶ which takes into account the entropy contribution to the free energy due to thermal fluctuations of vortices. $m(T)$ curves were, therefore, measured at different $H\parallel c$ in the 1 T SQUID, which showed the characteristic crossing point at a certain temperature T^* , as can be seen in Fig. 2. These data were used to calculate $M(\ln \mu_0 H)$

TABLE I. Transition temperatures and widths for the two samples analyzed as well as zero-field critical current densities (before and after neutron irradiation in the case of W002).

Sample	T_c (K)	ΔT_c (K)	$J_c(0 \text{ T}, 10 \text{ K})$ (A m ⁻²)
H5a	108.3	3.3	7.3×10^9
W002 unirradiated	107.6	2.4	3.00×10^{10}
W002 irradiated	106.7	2.5	4.86×10^{10}

for different temperatures, which was fitted linearly in order to obtain the slope of the magnetization. The penetration depth $\lambda_{ab}(T)$ was then deduced from $\partial M / \partial \ln \mu_0 H$ using Eq. (2) from Ref. 7, which is based on the Bulaevskii model. With $M(H)$ and $\lambda_{ab}(T)$ the upper critical field $H_{c2}(T)$ parallel to the c axis could be obtained via Eq. (6) of the same publication. All other reversible parameters were then deduced from the anisotropic Ginzburg-Landau relations.

E. Neutron irradiation

Neutron irradiation of one of our samples (W002) was performed in the central irradiation facility of the TRIGA-MARK-II research reactor in Vienna,⁸ during which it was exposed to a fast neutron fluence ($E > 0.1$ MeV) of $2 \times 10^{21} \text{ m}^{-2}$. Studies of YBCO and Bi-2212 single crystals^{9,10} showed that this fluence produces defect cascades with a density of $\sim 1 \times 10^{22} \text{ m}^{-3}$. They consist of spherical amorphized regions, 2–5 nm in diameter, which corresponds well to the superconducting coherence length in the ab plane of Bi-2223 over a broad temperature range. These defects can, thus, act as effective pinning centers. In addition to the cascades smaller defects, like point defects, are induced.

III. RESULTS AND DISCUSSION

A. Critical temperature

T_c and the transition widths ΔT_c (defined as the temperature difference between 10% and 90% of the Meissner value) before and after irradiation are listed in Table I. Neutron irradiation reduced T_c of sample W002 by less than 1 K. This decrease, corresponding to 4.5 K per 10^{22} m^{-2} , is very similar to the slope found in Ref. 11 for $\text{Tl}_2\text{Ca}_2\text{Ba}_2\text{Cu}_3\text{O}_{10}$ single crystals at *higher* neutron fluences. We did not observe the plateau reported in this study at the lowest fluence analyzed ($2 \times 10^{21} \text{ m}^{-2}$, i.e., the same as in our case). For polycrystalline (Bi,Pb)-2223 exposed to a neutron fluence of $2.4 \times 10^{21} \text{ m}^{-2}$ a stronger decrease in T_c by 2 K was found.¹² $\text{YBa}_2\text{Cu}_3\text{O}_7$ on the other hand showed a smaller effect of irradiation on the transition temperature with a reduction of only $1.74 \times 10^{-22} \text{ K m}^2$.¹³

The decrease in T_c after neutron irradiation has been explained by an increased number of point defects¹³ (oxygen vacancies) and is expected from impurity scattering in d -wave superconductors.¹⁴ The fact that our sample H5a showed a slightly higher T_c is, therefore, consistent with it having a lower density of growth-related defects, as indicated by its comparably low value of J_c .

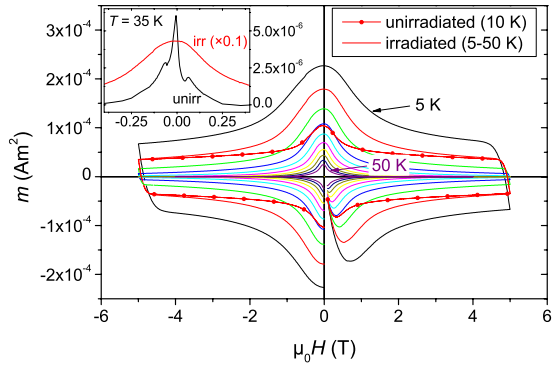


FIG. 3. (Color online) Magnetic moment vs field ($H\parallel c$) of sample W002 after irradiation ($T=5-50$ K, in 5 K steps), together with one curve for the unirradiated sample (10 K). The inset shows the second peak in $m(H)$ at $T=35$ K, which disappears after irradiation (the irradiated data have been scaled by a factor of 0.1).

B. Hysteresis loops and critical current densities

Figure 3 shows magnetic hysteresis loops for sample W002 after neutron irradiation measured at different temperatures in the VSM. For comparison a curve measured on the unirradiated sample at 10 K is also depicted to show the increase in magnetic moment due to the introduction of pinning centers by irradiation. From 35 K upward the curves show reversible parts.

The magnetic moment of W002 vs field at $T=35$ K measured in the 1 T SQUID is presented in the inset of Fig. 3. A second peak is clearly visible at $\mu_0H \approx \pm 60$ mT. This phenomenon, which has been explained by an order-disorder phase transition from the low-field Bragg glass to the high-field vortex glass, has been reported previously for Bi-2223 single crystals.¹⁵ The second maximum disappears after irradiation, a behavior which has also been observed in YBCO.¹⁶

The critical current density vs applied field, which was calculated from VSM $m(H)$ curves as described above, can be seen in Fig. 4. At higher temperatures neutron irradiation increases J_c over the whole field range. For 10 K, however, the curves for the unirradiated and the irradiated samples merge at a field of about 5 T, and also at 20 K we find a similar trend.

This can be understood as follows. At low fields defect cascades introduced by neutron irradiation act as strong pin-

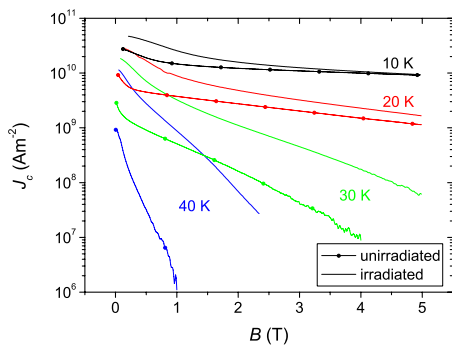


FIG. 4. (Color online) The critical current densities at different temperatures, which were derived from magnetic hysteresis loops of sample W002 before and after irradiation.

ning centers at all temperatures. As B increases we expect them to become less effective; the fluence to which W002 was exposed results in a defect distance similar to the vortex spacing at a field of only 1 T. Nevertheless, we find a strong J_c enhancement at elevated fields and temperatures. Also, the irreversibility line is shifted to higher values (at least at $T > 20$ K and the fields accessible to our measurements; see below). We conclude that, because of thermal activation, vortices cannot be pinned effectively by the small defects found in the pristine sample in this B and T range. Defect cascades introduced by neutron irradiation on the other hand act as strong pinning centers, despite their comparably small density.

At low temperatures defects already present in the pristine crystal pin flux lines effectively and the possible increase in J_c at high B due to irradiation is limited. It should be noted, however, that this is only true for the *relative* enhancement. Even at higher fields, like 4 T, J_c rises by a larger amount at 10 and 20 K, where of course the absolute values are higher, than it does at elevated temperatures. At 5 T we find the peculiar behavior that relative and absolute increases are higher at 20 than at 10 K. This is clearly caused by the growth-related defects being superior to defect cascades at low T and high B , due to their higher number, hence allowing little room for enhancement at 10 K and 5 T. An increase in J_c has also been reported after proton irradiation of Bi-2223 single crystals,¹⁷ as well as after neutron irradiation of Bi-2223 and (Bi,Pb)-2223 tapes.^{18,19}

The critical current densities of sample W002 before irradiation are slightly higher than those reported for an optimally doped crystal in Ref. 15. The deviations could be explained by variations in oxygen doping and defect densities as well as by the different evaluation formulas used. Our J_c values match more closely those reported in Ref. 20. The data in both studies^{15,20} have been obtained from magnetic measurements on single crystals produced in the same way as our samples.

H5a on the other hand gave smaller values, in particular at low temperatures, which could be explained by a smaller defect density in this pristine sample. Its critical current density vs field at 20 K corresponds well to values obtained from a Bi-2223 tape using SQUID magnetometry (sample 4 in Ref. 21, heat treated at ambient pressure). Even at low fields the tape's J_c is not suppressed with respect to the single crystal. This implies that over the whole field range the major contribution to its magnetic moment comes from intragranular rather than *intergranular* currents. Consequently also its J_c , deduced from magnetization measurements, is not limited by grain boundaries at low fields. It needs to be pointed out, however, that the transport J_c most likely is governed by the properties of the boundaries, not the grains.

At zero applied field and 40 K J_c of both our unirradiated samples is very similar to the data obtained by transport measurements²² on a Bi-2223 tape doped with ²³⁵U. Irradiation with thermal neutrons causes the fission of uranium creating randomly oriented linear defects, which seem to have a very similar effect on pinning as defect cascades due to fast neutron irradiation.^{18,19} This was also observed in a study conducted on YBa₂Cu₃O₇ bulk samples²³ and explained by the similar interaction volume of a single flux line with either

a collision cascade or a fission track. It is reasonable to expect the same behavior in Bi-2223 since pinning by both kinds of defects should gain the whole condensation energy of a pancake. At low fields the macroscopic critical current density of tapes is, in general, limited by the properties of grain boundaries, rather than grains.²² J_c , therefore, is suppressed at low B in tapes after irradiation because of damage incurred by the grain boundaries from neutrons.^{18,19,22} The single crystal of course did not suffer from this, which is why it showed a higher J_c than the tape in this field range after irradiation. At fields above ~ 0.5 T the fission tracks led to an enhancement, however by a significantly smaller amount than was the case after irradiation of our single crystal. Both the pristine and the irradiated tape showed a weaker field dependence; hence, their J_c exceeds that of the unirradiated single crystal for $B > 0.1$ T. This behavior can be attributed to the different measurement techniques used and the higher number of defects present in an unirradiated tape compared to a single crystal, which is due to the different production processes. Consequently, the tape surpasses our irradiated sample at fields above ~ 1.5 T.

Chu and McHenry¹⁷ conducted a study of proton irradiation of Bi-2223 single crystals, which leads to the fission of Bi atoms causing columnar damage with a preferential direction parallel to the incident beam.²⁴ Even aligned defects, however, were found to lead to isotropic pinning;²⁵ thus, the effect on J_c of defects caused by fission of Bi can be expected to be akin to those created by fission fragments of ²³⁵U. The latter defects in turn have similar pinning properties as defect cascades due to fast neutron irradiation, as mentioned above.²³ In Ref. 17 an increase by a factor of about 3 of self-field J_c at 20 and 40 K due to proton irradiation is reported. Whereas at the lower temperature we found a similar enhancement factor for our sample, we obtained a value of 13 at 40 K. We attribute this difference to two factors. First Chu and McHenry performed their measurements on an ensemble of 472 tiny single crystals, with their small size leading to a lower self-field and thus a higher J_c . Consequently, their values are comparable to ours only to a limited extent. Second their samples were grown in molten salt flux of KCl and are supposed to have a large amount of defects and impurities, as confirmed by the wide transition they exhibit. The enhancement factor due to irradiation depends strongly on the number and type of defects in the pristine samples. Bigger defects present before irradiation can lead to an increased J_c even at elevated temperatures; thus, a smaller enhancement is found.

The dependence of J_c on temperature is presented in Fig. 5, which illustrates that the relative increase due to irradiation is stronger at higher temperatures. As explained earlier the reason for this is pinning centers in the pristine sample being less effective at higher temperatures, thus allowing more potential for enhancement by irradiation in this regime.

C. Irreversibility line

Figure 6 shows the irreversibility lines for sample H5a (unirradiated) and for W002 (after irradiation). A few points measured on W002 before irradiation corresponded well to

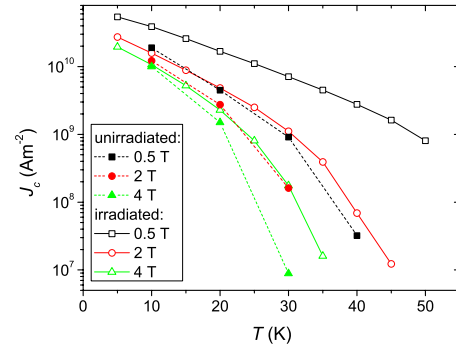


FIG. 5. (Color online) The temperature dependence of the critical current density of sample W002 for fields of 0.5, 2, and 4 T before and after irradiation.

the values for H5a, thus allowing us to determine the effects of neutron irradiation by comparing H5a to W002 after irradiation.

Not surprisingly the curve for our unirradiated sample replicates well the data of Piriou *et al.*¹⁵ which were obtained from a very similar optimally doped single crystal by the same method. After neutron irradiation the irreversibility line of W002 shifted to higher values, a behavior reported previously for Bi-2223 tapes²⁶ and polycrystalline (Bi,Pb)-2223.¹² In the latter study a sample was irradiated to a similar neutron fluence as in the present work and the values for the irreversibility field show qualitatively the same behavior as our data, whereas the absolute values are somewhat higher. This is at least partly due to different evaluation methods employed. The data from Ref. 26 were obtained from transport measurements, which means that they cannot be quantitatively compared to ours. In another study²¹ the irreversibility line of a pristine tape was measured using SQUID magnetometry, which led to higher values compared to those of our sample before irradiation. The irreversibility line of their sample 4 is virtually identical over the whole temperature range investigated to the curve for our single crystal *after* irradiation.²¹ Again, at least to a certain extent, we at-

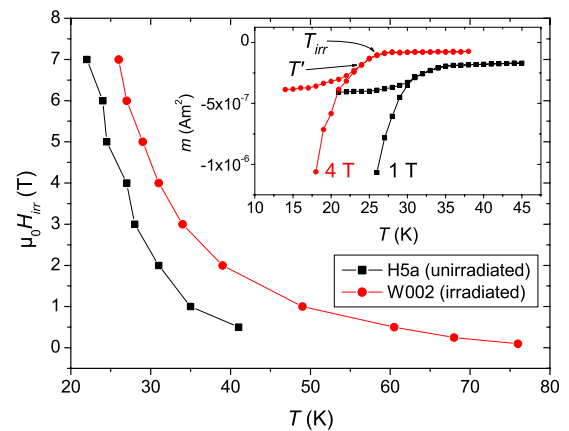


FIG. 6. (Color online) The irreversibility line for samples H5a (unirradiated) and W002 (irradiated) for $H \parallel c$. The inset shows $m(T)$ curves of H5a used to determine the irreversibility temperature for respective fields using the kink at T_{irr} , not the drifting apart of fc and zfc curves at T' (see text).

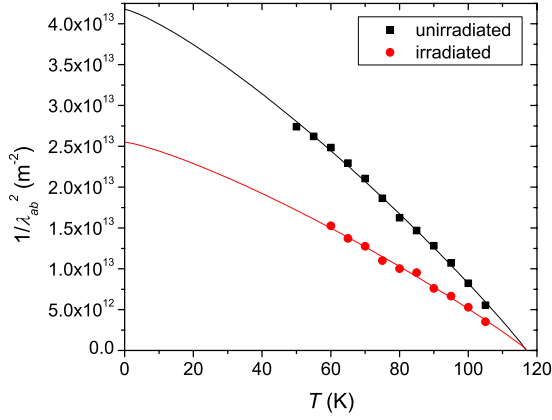


FIG. 7. (Color online) The penetration depth as measured before and after neutron irradiation. The lines are a fit to the BCS relation with both $\lambda_{ab}(0)$ and T_{c0} varied.

tribute these deviations to different evaluation methods, but also to a higher defect density in the pristine tape.

D. Reversible properties

For sample W002 and $H\parallel c$ the crossing point in the $m(T)$ curves which were used to obtain the reversible properties was found at $T^* = 108.1$ K before and at 107.5 K after irradiation. The penetration depth λ_{ab} was calculated as described above. Figure 7 shows $1/\lambda_{ab}^2$ plotted vs temperature together with fits to the BCS relation for d -wave superconductors,

$$\lambda_{ab}(T) = \lambda_{ab}(0)[1 - (T/T_{c0})^{1.25}]^{-0.47}. \quad (1)$$

T_{c0} is the mean-field transition temperature,⁶ compared to the critical temperature T_c which has been deduced from ac susceptibility measurements (see above). A very good fit was obtained when both $\lambda_{ab}(0)$ and T_{c0} were used as fitting parameters. This, however, led to values of $\lambda_{ab,1}(0)$ and $T_{c0,1}$, which are not consistent with Eq. (16) from Ref. 6 and the measured T^* . We, therefore, used the latter equation to calculate T_{c0} from T^* and the interlayer distance s , as determined from the crossing point in $m(T)$, and an estimated value of $\lambda_{ab}(0)$. A fit with the so obtained T_{c0} held constant gave a new $\lambda_{ab}(0)$, which was then used to calculate T_{c0} again. This procedure was repeated until the values remained constant. While this led to very similar values for the penetration depth [$\lambda_{ab,2}(0)$], the transition temperature obtained in this way ($T_{c0,2}$) appears to be more realistic. The quality of the fit to the measured $1/\lambda_{ab}^2(T)$, however, is worse. All values of $\lambda_{ab}(0)$ and T_{c0} can be found in Table II.

When the sample was irradiated the penetration depth at $T=0$ K increased by a factor of about 1.3. This factor can be used to scale the unirradiated to the irradiated data over the whole temperature range analyzed. An increased value of λ_{ab} after neutron irradiation has been reported previously¹² for (Bi,Pb)-2223 and is also consistent with theoretical predictions for the penetration depth in s - and d -wave superconductors.^{27–29} From these models, however, a significantly smaller influence of impurity scattering would be expected ($\sim 5\%$ reduction in $1/\lambda_{ab}^2$) than that found in our mea-

TABLE II. Reversible parameters of sample W002 at $T=0$ K before and after neutron irradiation together with the respective values of T_{c0} obtained from the fits. T^* is the temperature of the crossing point in the $m(T)$ curves.

	Unirradiated	Irradiated
T^* (K)	108.1	107.5
$\lambda_{ab,1}$ (nm)	155	198
$T_{c0,1}$ (K)	116.9	117.3
$\lambda_{ab,2}$ (nm)	151	192
$T_{c0,2}$ (K)	113.3	113.2
$\mu_0 H_{c2,fit}$ (T)	113	175
$T_{c0,Hc2}$ (K)	111.8	109.9
$\mu_0 H_{c2,BCS}$ (T)	113	190
ξ_{ab} (nm)	1.7	1.4
$\mu_0 H_{c,GL}$ (T)	0.90	0.89
$\mu_0 H_{c,fit}$ (T)	0.74	0.70
$T_{c0,Hc}$ (K)	111.8	111.2

surements ($\sim 40\%$), given the small decrease in T_c of our samples after irradiation.

In a next step we deduced the upper critical field, which is depicted in Fig. 8. The data were fitted to

$$H_{c2}(T) = H_{c2}(0)[1 - (T/T_{c0})^{1.5}], \quad (2)$$

and the fit parameters $H_{c2,fit}(0)$ and $T_{c0,Hc2}$ can again be found in Table II. Unlike in the case of λ_{ab} the obtained values for the transition temperature T_{c0} appear plausible. At 0 K H_{c2} increased by a factor of about 1.5, which again scales the two curves to each other for all $T < T_{c0}$.

Similar values as those obtained from the fit to Eq. (2) were found for the upper critical field at $T=0$ K using the BCS relation for the clean limit,³⁰

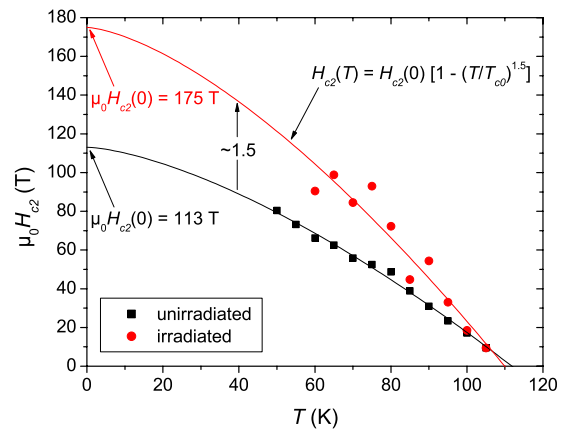


FIG. 8. (Color online) Upper critical field vs temperature for sample W002 and $H\parallel c$. The data were fitted with both $H_{c2}(0)$ and T_{c0} varied.

$$H_{c2,BCS}(0) = -0.73T_c \left. \frac{dH_{c2}}{dT} \right|_{T=T_{c0}}, \quad (3)$$

as can be seen in Table II. The three points closest to T_{c0} were fitted linearly in order to obtain the slope of H_{c2} at $T=T_{c0}$.

Ossandon *et al.*¹² also reported an increase in the upper critical field after neutron irradiation of the (Bi,Pb)-2223 sample they studied. As in the present work they employed the Bulaevskii model⁶ to obtain the reversible parameters and they explained the increases in both λ_{ab} and H_{c2} by a reduction in the mean-free path for conduction electrons due to radiation damage. We do not believe that our results can be explained by this effect alone. For a 50% increase in H_{c2} an unrealistically short mean free path $l \approx 2\xi^{cl}$ would be required according to

$$H_{c2} = H_{c2}^{cl}(1 + \xi^{cl}/l). \quad (4)$$

ξ is the coherence length and the superscript ‘‘cl’’ indicates the clean limit.

For *d*-wave superconductors a *decrease* in the upper critical field due to impurity scattering was predicted.^{31–33} Consequently, these theoretical studies are in contradiction to our findings for H_{c2} . They were, however, confirmed by experiments, using YBCO samples irradiated by electrons or doped with Zn or Pr.

The discrepancy between our results and the above theories^{31–33} can be explained in two ways. The Bulaevskii model only applies to sufficiently anisotropic superconductors, like Bi-2212.⁷ The 2223 phase shows a lower anisotropy compared to Bi-2212,¹⁵ and therefore the model might not describe Bi-2223 correctly, potentially leading to unreliable values of H_{c2} . This would explain why both our data and the results presented in Ref. 12 (which were also deduced from the Bulaevskii model) disagree with theoretical predictions for the upper critical field. It should be pointed out, however, that the $m(\ln H)$ curves became significantly flatter after irradiation. Linear extrapolation thus leads to higher values of $H(m=0)$, which indicates an increased H_{c2} , independent of any model.

We therefore conclude that, while impurity scattering as discussed in Refs. 31–33 might also play a role, the strong increase in H_{c2} must be due to a different mechanism, possibly but not necessarily based on impurity scattering. One explanation would be a reduced Fermi velocity

$v_F \propto \xi^{cl} \propto 1/\sqrt{H_{c2}}$ after irradiation. This could be due to a decreased charge carrier density or a smearing of the Fermi surface. The first case is unlikely, however, as it would also have a significant impact on T_c . The latter would make the Fermi surface more isotropic and thus cause a smaller in-plane value of v_F .

We then used the values of $H_{c2,fit}(0)$ to calculate the *ab*-plane coherence lengths $\xi_{ab}(0)$ from the Ginzburg-Landau relation $\mu_0 H_{c2} = \Phi_0 / 2\pi \xi_{ab}^2$. After irradiation $\xi_{ab}(0)$ had decreased by 20%.

The thermodynamic critical field $H_{c,GL}$ at 0 K followed from the values of $\xi_{ab}(0)$ and $\lambda_{ab,2}(0)$ and the Ginzburg-Landau relation $\mu_0 H_c = \Phi_0 / 2^{3/2} \pi \xi_{ab} \lambda_{ab}$. H_c was not changed significantly by irradiation (see Table II). This behavior is expected as $H_c \propto \Delta(0) \propto T_c$ [where $\Delta(0)$ is the energy gap at $T=0$ K] and T_c has not changed notably. For comparison the thermodynamic critical field was calculated from ξ_{ab} and λ_{ab} at $T>0$ K and fitted to

$$H_c(T) = H_c(0)[1 - (T/T_{c0})^2], \quad (5)$$

which gave $H_{c,fit}(0)$ and T_{c0,H_c} . While $H_{c,fit}(0)$ is somewhat smaller than $H_{c,GL}(0)$ it again is not significantly affected by radiation damage.

IV. CONCLUSIONS AND SUMMARY

We have conducted magnetic measurements on Bi-2223 single crystals before and after irradiation with fast neutrons. While the transition temperature remained almost constant, we found an increase in the critical current density and the irreversibility line due to the crystal defects introduced by irradiation. This behavior is in agreement with irradiation experiments on BSCCO tapes and single crystals using protons and neutrons.

The reversible properties were determined using a model which takes vortex fluctuations into account. Both the penetration depth and the upper critical field had increased after irradiation. An increase in λ_{ab} is qualitatively consistent with theoretical predictions for impurity scattering in *s*- and *d*-wave superconductors. H_{c2} in *d*-wave superconductors, on the other hand, would be expected to become lower when the defect density increases. We, therefore, conclude that the introduced defects cause additional phenomena which have a stronger influence on the reversible parameters than that predicted by the above theoretical models alone.

*eisterer@ati.ac.at

¹T. Fujii, T. Watanabe, and A. Matsuda, *J. Cryst. Growth* **223**, 175 (2001).

²B. Liang, C. T. Lin, P. Shang, and G. Yang, *Physica C* **383**, 75 (2002).

³E. Giannini, V. Garnier, R. Gladyshevskii, and R. Flükiger, *Supercond. Sci. Technol.* **17**, 220 (2004).

⁴C. P. Bean, *Phys. Rev. Lett.* **8**, 250 (1962).

⁵A. Schilling, H. R. Ott, and T. Wolf, *Phys. Rev. B* **46**, 14253

(1992).

⁶L. N. Bulaevskii, M. Ledvij, and V. G. Kogan, *Phys. Rev. Lett.* **68**, 3773 (1992).

⁷V. G. Kogan, M. Ledvij, A. Y. Simonov, J. H. Cho, and D. C. Johnston, *Phys. Rev. Lett.* **70**, 1870 (1993).

⁸H. W. Weber, H. Böck, E. Unfried, and L. R. Greenwood, *J. Nucl. Mater.* **137**, 236 (1986).

⁹M. C. Frischherz, M. A. Kirk, J. Farmer, L. R. Greenwood, and H. W. Weber, *Physica C* **232**, 309 (1994).

- ¹⁰M. Aleksa, P. Pongratz, O. Eibl, F. M. Sauerzopf, H. W. Weber, T. W. Li, and P. H. Kes, *Physica C* **297**, 171 (1998).
- ¹¹G. Brandstätter, F. M. Sauerzopf, and H. W. Weber, *Phys. Rev. B* **55**, 11693 (1997).
- ¹²J. G. Ossandon, J. R. Thompson, Y. C. Kim, Y. R. Sun, D. K. Christen, and B. C. Chakoumakos, *Phys. Rev. B* **51**, 8551 (1995).
- ¹³F. M. Sauerzopf, H. P. Wiesinger, H. W. Weber, and G. W. Crabtree, *Phys. Rev. B* **51**, 6002 (1995).
- ¹⁴A. J. Millis, S. Sachdev, and C. M. Varma, *Phys. Rev. B* **37**, 4975 (1988).
- ¹⁵A. Piriou, Y. Fasano, E. Giannini, and Ø. Fischer, *Phys. Rev. B* **77**, 184508 (2008).
- ¹⁶M. Werner, F. M. Sauerzopf, H. W. Weber, and A. Wisniewski, *Phys. Rev. B* **61**, 14795 (2000).
- ¹⁷S. Chu and M. E. McHenry, *Physica C* **337**, 229 (2000).
- ¹⁸G. W. Schulz, C. Klein, H. W. Weber, H. W. Neumüller, R. E. Gladyshevskii, and R. Flükiger, *Inst. Phys. Conf. Ser.* **158**, 1105 (1997).
- ¹⁹Q. Y. Hu, H. W. Weber, F. M. Sauerzopf, G. W. Schulz, R. M. Schalk, H. W. Neumüller, and S. X. Dou, *Appl. Phys. Lett.* **65**, 3008 (1994).
- ²⁰N. Clayton, N. Musolino, E. Giannini, V. Garnier, and R. Flükiger, *Supercond. Sci. Technol.* **17**, S563 (2004).
- ²¹M. Kiuchi, S. Takayama, E. S. Otabe, T. Matsushita, J. Fujikami, K. Hayashi, and K. Sato, *Physica C* **463**, 825 (2007).
- ²²S. Tönies, H. W. Weber, Y. C. Guo, S. X. Dou, R. Sawh, and R. Weinstein, *Appl. Phys. Lett.* **78**, 3851 (2001).
- ²³M. Eisterer, S. Tönies, W. Novak, H. W. Weber, R. Weinstein, and R. Sawh, *Supercond. Sci. Technol.* **11**, 1001 (1998).
- ²⁴L. Krusin-Elbaum, J. R. Thompson, R. Wheeler, A. D. Marwick, C. Li, S. Patel, D. T. Shaw, P. Lisowski, and J. Ullmann, *Appl. Phys. Lett.* **64**, 3331 (1994).
- ²⁵F. Hillmer, G. Jakob, P. Haibach, U. Frey, T. Kluge, H. Adrian, G. Wirth, E. Jäger, and E. Schimpf, *Physica C* **311**, 11 (1999).
- ²⁶S. Tönies, H. W. Weber, Y. C. Guo, S. X. Dou, R. Sawh, and R. Weinstein, *IEEE Trans. Appl. Supercond.* **11**, 3904 (2001).
- ²⁷L. S. Borkowski and P. J. Hirschfeld, *Phys. Rev. B* **49**, 15404 (1994).
- ²⁸H. Kim and E. J. Nicol, *Phys. Rev. B* **52**, 13576 (1995).
- ²⁹Y. Sun and K. Maki, *Phys. Rev. B* **51**, 6059 (1995).
- ³⁰T. P. Orlando, E. J. McNiff, S. Foner, and M. R. Beasley, *Phys. Rev. B* **19**, 4545 (1979).
- ³¹H. Won and K. Maki, *Physica B* **199-200**, 353 (1994).
- ³²H. Won and K. Maki, *Physica C* **282-287**, 1837 (1997).
- ³³J. Y. Lin, S. J. Chen, S. Y. Chen, C. F. Chang, H. D. Yang, S. K. Tolpygo, M. Gurvitch, Y. Y. Hsu, and H. C. Ku, *Phys. Rev. B* **59**, 6047 (1999).